

Introduction

In general, marine data always contain strong surface-related multiples, which are usually treated as noise. Despite its usual classification as noise, energy from multiples often penetrates into the target where primaries are weakly focused. For example, in subsalt regions, multiples can provide more detailed information than from primary imaging alone. Moreover the reflection angles of multiples are always smaller than those of the primaries, and smaller reflection angles provide higher vertical resolution. Based on these advantages, Liu et al. (2011) proposed multiples reverse time migration, similar to that of Jiang et al. (2007) who used the Kirchhoff method or Muijs et al. (2005) who used phase-shift migration. They transform each hydrophone into a virtual point source with a time history equal to that of the recorded data. These virtual sources are used to numerically generate downgoing wavefields that are correlated with the back-projected surface-related multiples to give the migration image. We will refer to the Liu et al. (2011) method as multiples RTM (MRTM).

However, multiples RTM only gives the correct noise-free image when the downgoing (N-1)th-order multiple correlate with the back-propagated Nth-order multiple of the input data. Otherwise, there will be crosstalk in the migration image. To overcome this problem, we propose multiples least-squares reverse time migration (MLSRTM) which can partly improve the image quality by reducing migration artifacts, balancing amplitudes and suppressing crosstalk (Dai et al., 2010, 2012).

Theory

Multiples reverse time migration

Liu et al. (2011) proposed multiples reverse time migration (MRTM) to improve the image under a salt body. Compared to conventional RTM in which the source is an impulsive wavelet and the input data mostly contain primaries, the recorded trace becomes the time history of a virtual point source at that hydrophone, and the back-propagated data are the first-order and higher-order surface related multiples. Different from conventional RTM that uses the primary only, MRTM uses all orders of surface related multiples that will generate the crosstalk. Figure 1 shows the table with the non-diagonal imaging conditions that are the causative agents for crosstalk. Here, the primary is defined as the zeroth-order multiple. Propagation of the (N-1)th-order downgoing multiple as the virtual source will generate the Nth-order multiple received by the hydrophone. Hence, zero-lag cross-correlation of the forward-propagated (N-1)th-order multiple as the virtual source with the back-propagated wavefield of the Nth-order multiple will give the correct image. When the virtual source is the (N-1)th-order multiple and the back-projected multiple is higher than the Nth-order, the migration imaging condition will produce crosstalk noise. For example, the (N+1)th-order multiple is incorrectly treated as the Nth-order multiple so that these multiple reflections will be incorrectly imaged. When the virtual source wavefield is a downgoing (N-1)th-order multiple and the back-projected multiple is lower than Nth-order, the time of the back-propagated wavefield always appears later than the time of the forward-propagated wavefield. Therefore, these two wavefields will not meet anywhere for coherent imaging.

Multiples least-squares reverse time migration

As shown in Figure 1, there is crosstalk noise originating from the correlation of downgoing source fields that are less than one order different than the order of the back-propagated multiples. In order to suppress these artifacts, we apply the least-squares migration technology to the data.

The misfit function is defined as:

$$f(\mathbf{m}) = \frac{1}{2} \|\mathbf{L}\mathbf{m} - \mathbf{M}\|^2, \quad (1)$$

where, \mathbf{m} is the reflectivity model, \mathbf{L} is the Born modeling operator that predicts multiples and \mathbf{M} is the recorded surface-related multiples. The reflectivity distribution can be iteratively updated by the, for

Imaging Conditions for MRTM

receivers sources	1th-order multiple	2th-order multiple
primary	image	artifact	artifact
1th-order multiple	no image	image	artifact
2th-order multiple	no image	no image	image
.....			

Figure 1 Imaging conditions for MRTM. Different imaging conditions result from multiplying the spectra of the downward propagating source field (one of the terms in the far-left column) by the back-propagated reflection field (one of the terms in the top row) and summing over all frequencies to get the migration result listed in the matrix.

example, steepest descent method:

$$\mathbf{m}^{k+1} = \mathbf{m}^k - \alpha \mathbf{g}^k, \quad (2)$$

$$\alpha = \frac{(\mathbf{g}^k)^T \cdot \mathbf{g}^k}{(\mathbf{L}\mathbf{g}^k)^T \cdot \mathbf{L}\mathbf{g}^k}, \quad (3)$$

where, k is the iteration number and α is the step length, and \mathbf{g} is the misfit gradient. In each iteration, the residual multiples are migrated by reverse time migration to compute the gradient and the reflectivity is updated by the steepest descent method with the step length α . The iterative procedure is stopped when the data residual falls below a specified limit.

Generation of multiples

In MLSRTM, the predicted data are the surface-related multiples, so their accurate calculation is crucial for the success of this method. To achieve this goal, we use Born modeling to calculate the predicted surface-related multiples. Recalling the Born modeling approximation (Stolt and Benson., 1986), an element of the vector \mathbf{M} can be written in the frequency domain as:

$$M(\mathbf{x}_g, \mathbf{x}_s) = 2\omega^2 \int \overbrace{m(\mathbf{x})G(\mathbf{x}|\mathbf{x}_g)}^{\text{upgoing}} \overbrace{\int G(\mathbf{x}|\mathbf{x}'_g)d(\omega, \mathbf{x}'_g, \mathbf{x}_s)d\mathbf{x}'_g d\mathbf{x}}^{\text{downgoing}}, \quad (4)$$

where, ω is the frequency, and $m(\mathbf{x})$ is the element of the reflectivity vector \mathbf{m} , \mathbf{x} is the location of the subsurface point, \mathbf{x}_s and \mathbf{x}_g are the source and geophone locations, $G(\mathbf{x}|\mathbf{x}'_g)$ is the Green's function for a source at \mathbf{x}'_g and an observer at \mathbf{x} in the background velocity model, $G(\mathbf{x}|\mathbf{x}_g)$ is the Green's function for a source at \mathbf{x}_g and an receiver at \mathbf{x} , and $d(\omega, \mathbf{x}'_g, \mathbf{x}_s)$ represents the spectrum of the recorded trace that serves as the time history of the virtual source at \mathbf{x}'_g which includes both primaries and surface-related multiples.

Numerical example

Sigsbee2B model

The Sigsbee2B salt model is discretized into a 600×1600 grid with a gridpoint separation of 10 m. A fixed-spread acquisition geometry is used and there are 400 shots with a 40 m shot interval and

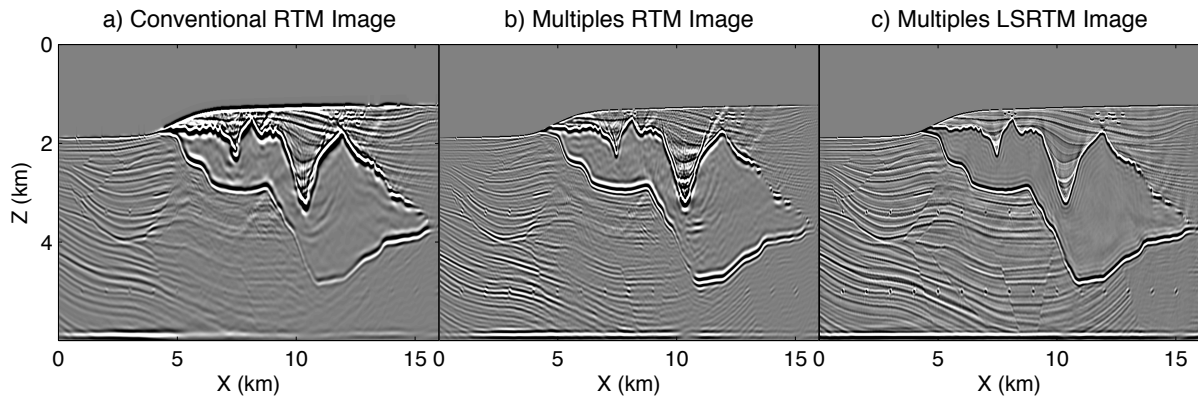


Figure 2 a) Conventional RTM image. b) Multiples RTM image. c) MLSRTM image after 30 iterations.

800 geophones spaced at 20 m covering the entire surface. For MRTM and MLSRTM, the smooth velocity model is used as the migration velocity. Applying MRTM to this synthetic data set results in the migration image shown in Figure 2b. Compared to the conventional RTM image in Figure 2a, MRTM has the advantages of higher vertical resolution and wider subsurface illumination, especially under the salt body. However, there is crosstalk in some places for the reasons discussed in the previous section. To suppress the crosstalk, we apply MLSRTM to these synthetic data, and Figure 2c shows the MLSRTM image after 30 iterations. Compared to the MRTM image in Figure 2b, the MLSRTM image shows less crosstalk, more balanced amplitudes, and higher resolution. An advantage of MLSRTM compared to conventional LSRTM is that knowledge of the source wavelet is not required. Additionally, the MRTM image is the sum of the diagonal elements of the matrix shown in Figure 1, so that the signal-to-noise ratio of the final image MLSRTM might be greatly enhanced, compared to conventional LSM that only migrates the primaries. This assumes that the crosstalk noise has been sufficiently suppressed in the least squares migration, which will not be the case if the accuracy of the migration velocity model is inadequate.

Gulf of Mexico data

In this section, multiples least-squares reverse time migration is applied to streamer data acquired from the Gulf of Mexico with a shot interval of 26.67 m, with 180 active hydrophones per shot for a total of 1001 shot gathers. The source-receiver near offset is 106.68 m and the far offset is about 4.77 km with the hydrophone interval of 26.67 m.

Prior to application of the MRTM or MLSRTM methods, the surface-related multiples are predicted by a two-step SRME method. The first step is the prediction of multiples by the convolution of the data set. The second step is to use a prediction-error filter to subtract the multiples. The MRTM images are shown in Figures 3b, and compared to the conventional RTM image in Figure 3a the MRTM image appears to show a higher vertical resolution and more details under the salt body. Figure 3c shows the MLSRTM image after 30 iterations. Compared to the MRTM image in Figure 3b, the MLSRTM image appears to have higher subsalt resolution and fewer artifacts in the salt body. Unfortunately the subsurface ground truth was not available to correctly judge which result was correct.

Conclusions

We propose multiples least-squares reverse time migration to suppress the crosstalk in multiples reverse time migration. In this method, recorded traces are used as the time histories of the virtual sources at the hydrophones and the surface-related multiples are the observed data. Tests on synthetic Sigsbee2B data and field data from the Gulf of Mexico demonstrate that MLSRTM can effectively suppress the crosstalk in the final image. Compared to conventional LSM, the advantages of MLSRTM are that no knowledge

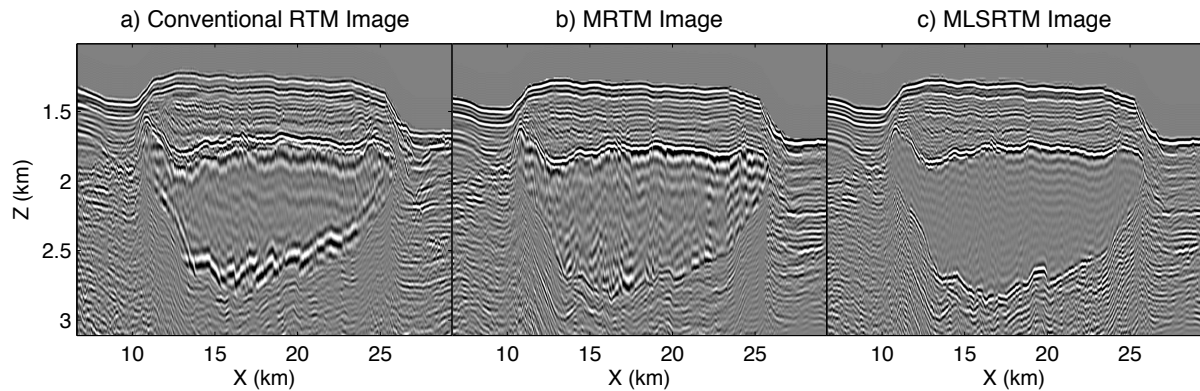


Figure 3 a) Conventional RTM image. b) MRTM image. c) MLSRTM image of filtered multiples.

of the actual source wavelet is needed, and it migrates all orders of surface-related multiples to enhance the signal-to-noise ratio of the final image.

The limitation of MLSRTM is that it might be difficult to accurately predict the absolute amplitudes of the recorded multiples. Another disadvantage is that attenuation in the earth can significantly reduce the high frequency content of the surface-related multiple reflections, which will reduce resolution compared to imaging with primary reflections. This suggests that the Q distribution should first be estimated from the data and then should be accounted for in the forward and adjoint modeling of the multiples.

Acknowledgements

We thank the KAUST Supercomputing Lab for the computer cycles they donated to this project. We are especially grateful for the use of the SHAHEEN supercomputer. We also acknowledge the support of the CSIM sponsors (<http://csim.kaust.edu.sa>).

References

- Dai, W., Boonyasiriwat, C. and Schuster, G.T. [2010] 3D multi-source least-squares reverse time migration. *SEG Technical Program Expanded Abstracts*, **611**, 3120–3124, doi:10.1190/1.3513494.
- Dai, W., Fowler, P. and Schuster, G.T. [2012] Multi-source least-squares reverse time migration. *Geophysical Prospecting*, **60**(4), 681–695, ISSN 1365-2478, doi:10.1111/j.1365-2478.2012.01092.x.
- Jiang, Z., Sheng, J., Yu, J., Schuster, G.T. and Hornby, B.E. [2007] Migration methods for imaging different-order multiples. *Geophysical Prospecting*, **55**(1), 1–19, ISSN 1365-2478, doi:10.1111/j.1365-2478.2006.00598.x.
- Liu, Y., Chang, X., Jin, D., He, R., Sun, H. and Zheng, Y. [2011] Reverse time migration of multiples for subsalt imaging. *Geophysics*, **76**(5), WB209–WB216, doi:10.1190/geo2010-0312.1.
- Muijs, R., Holliger, K. and Robertsson, J.O.A. [2005] Prestack depth migration of primary and surface-related multiple reflections. *SEG Technical Program Expanded Abstracts 2005*, **537**, 2107–2110, doi:10.1190/1.2148128.
- Stolt, R.H. and Benson, A.K. [1986] *Seismic migration : theory and practice*, vol. 5. London : Geophysical Press, doi:10.1111/j.1365-2478.1994.tb00231.x.